



Thermo-environmental life cycle assessment of hydrogen production by autothermal reforming of bioethanol



Zouhour Khila^a, Ines Baccar^{a,b}, Intidhar Jemel^{a,b}, Noureddine Hajjaji^{a,*}

^a Unité de Recherche Catalyse et Matériaux pour l'Environnement et les Procédés URCMEP (UR11ES85), Ecole Nationale d'Ingénieurs de Gabès, Université de Gabès, Rue Omar Ibn Alkhattab, 6029 Gabès, Tunisia

^b Institut Supérieur des Etudes Technologiques de Gabès, Route de Medenine, 6011 Gabès, Tunisia

ARTICLE INFO

Article history:

Received 29 February 2016

Revised 23 November 2016

Accepted 29 December 2016

Available online xxxxx

Keywords:

Hydrogen

Bioethanol

Autothermal reforming

Exergy

Life cycle assessment

ABSTRACT

This paper proposes a methodology devoted to finding and selecting more accurate conditions for sustainable hydrogen production via autothermal reforming of bioethanol. This methodology implies entire hydrogen production process design and simulation, energetic, exergetic and environmental life cycle assessment analysis studies and parametric (intuitive and design of experiment based methods) investigations.

A base-case process operating under conditions recommended by simple investigation of chemical reactions was thoroughly studied. The results show that this base case process suffers from low performance. This is because the energetic, exergetic and environmental performances are comparatively lower than similar findings previously reported by other researchers for other reformates. The parametric investigation indicates that the process performances could be ensured by a proper and rational combination of the reactor temperature and the steam-to-carbon ratio. A key outcome of this research lies in establishing of second order mathematical models. These models can rapidly estimate the process performances (energetic, exergetic and environmental) based on temperature and the steam-to-carbon ratio.

This paper recommends a reforming a temperature of 800 °C and a steam-to-carbon ratio of 4 as the accurate conditions for autothermal reforming of bioethanol. Such conditions ensure not only the lowest consumption of energy to generate a given amount of hydrogen but also the best environmental performance of the entire system.

© 2017 International Energy Initiative. Published by Elsevier Inc. All rights reserved.

Introduction

Dependence on fossil hydrocarbon fuels as the main energy sources has led to not only serious energy crisis but also environmental pollutions. The only way to resolve these problems is to move towards alternative, renewable, efficient and cost-effective energy sources with less environmental impacts. Hydrogen is, currently, considered as one of the leading candidates in the search for an alternative to fossil fuels (FF). Nevertheless, H₂ is only an energy carrier like electricity and not a primary energy source. H₂ can be produced from a wide variety of energy sources, such as natural gas, coal, biomass, solar (thermal and photovoltaic), etc. (Martinez-Frias, 2003). Despite all the effort made, 96% of the produced H₂ in the world comes from FF, with a considerable amount of CO₂ produced emissions in these processes (Abánades et al., 2013). FF-to-H₂ system appears to have limited horizons, and the development and implementation of new methods for eco-friendly H₂ production, especially from biorenewable feedstocks, are

absolutely required. Therefore, there has been, recently, a significant amount of research going on to produce H₂ efficiently at low cost and minimum environmental impact from renewable sources.

Among various renewable feedstock alternatives for H₂ production, bioethanol has attracted much attention because of its relatively high H₂ content, availability, ease of storage, handling and safety, including its low comparative toxicity (Hou et al., 2015). Moreover, bioethanol can be produced renewably from several biomass sources such as (i) sugar or starch crops (sugar beet, sugar cane, corn and wheat, etc.), (ii) lignocellulosic biomass, and (iii) algae biomass (Lee and Kim, 2013). It should be noted that using H₂ from bioethanol is more efficient than bioethanol used directly in internal combustion engines and/or blended with gasoline (Seelam et al., 2012). The upgrading of raw bioethanol (crude bioethanol) requires various purification steps prior to be blended with gasoline or supplied to an internal combustion engine (Seelam et al., 2012). In fact, fuel grade bioethanol needs to be water-free. Thus the purification requires distillation beyond the azeotropic point, and this is one of the major production costs of fuel-grade ethanol, consuming almost 3/4 of the energy used in the bioethanol production process (Ni et al., 2007; Rass-Hansen et al.,

* Corresponding author.

E-mail address: Hajjaji.nour@gmail.com (N. Hajjaji).

2008; Mondal et al., 2015). Therefore, the use of raw bioethanol as a feedstock in H₂ production will minimize the heat consumption during the distillation process.

Several catalytic processes have been developed in recent years to convert bioethanol-to-H₂ by different routes, such as catalytic steam reforming (SR), partial oxidation (POX), autothermal reforming (ATR), CO₂ reforming, etc. Among these reforming processes, the ATR has received much attention in research during the recent years as a viable process for H₂ generation for fuel cell systems (Divins et al., 2013). ATR or, more generally denoted oxidative steam reforming, is a combination of SR and POX reactions. This combination is considered as one of the most attractive options for the on-board reforming of complex hydrocarbons. ATR has been suggested to ameliorate the difficulties of steam reforming. Specifically, autothermal reforming overcomes the steam reforming limitations of high temperature operations and fast dynamic responses. Additionally, an autothermal reformer can reduce the size, weight, start-up, shut-down, and other dynamic response times (Ahmed and Krumpelt, 2001). For these reasons, many efforts have been made to improve H₂ productivity in the ATR of ethanol. However, most of the efforts in this field have been focused on thermodynamic investigations of the bioethanol ATR reaction and/or researching catalysis in this system, but little attention has been devoted to the energetic and environmental performances of an entire system that includes all of the steps involved in the production of H₂ via ATR of bioethanol.

In recent decades, there has been an increasing interest in using both energy and exergy analysis modeling techniques for energy-utilization assessments. The energy analysis is the basic method of a process investigation. It is based on the first law of thermodynamics, which expresses the principle of the conservation of energy. Energy analysis has some inherent limitations, such as not accounting for degradation of the quality of energy through dissipative processes, and does not characterize the irreversibility of operations within the process (Wang et al., 2010). The exergy analysis is a modern thermodynamic method used as an advanced tool for process evaluation (Szargut et al., 1998). Based on both the first and the second laws of thermodynamics, exergy analysis compensates for the inability of the energy analysis to reveal the losses of energy due to its thermodynamic imperfections, and it plays unique roles in revealing the reasons for, location of and direction of improvement for losses. Therefore, exergy analysis has been widely used in recent years in assessing the performance of various bioenergy production processes. For example, Modarresi and colleagues (Modarresi et al., 2010) applied exergy analysis to a novel process for biological production of H₂ from biomass employing thermophilic and photo-heterotrophic bacteria. The authors obtained a chemical exergetic efficiency of 36–45% without considering any heat and process integration. In another study, Li and co-workers (Li et al., 2015) established a theoretical framework for the exergy analysis and advanced exergy analysis of a real biomass boiler. They showed that the maximum exergy destruction occurs in the combustion process, followed by the water walls and radiant superheater and the low temperature superheater. Most recently, Karellas and Braimakis (2015) have performed an energy–exergy analysis and economic investigation of a cogeneration and trigeneration organic Rankine cycle - vapor compression cycle hybrid system utilizing biomass fuel and solar power. Their results showed that, in the base case scenario, the net electric efficiency is 2.38%, with an electricity output equal to 1.42 kW_e and a heating output of 53.5 kW_{th}.

One of the most important criteria to inform decision-makers on the most sustainable options for process design is the evaluation of the environmental impacts. In this context, life cycle assessment (LCA) methodology could be used in parallel with the process design for finding and assessing technical solutions that could be adopted in the production process for reducing the environmental impacts (Hajjaji, 2014). LCA is a holistic method that assesses the impact of a product by considering all stages of its life cycle. LCA is considered as a “cradle to grave” method of assessing resource use and emissions to the environment from the extraction of resources through manufacturing, transportation, operation

and recycling or final disposal (Guinée et al., 2002). LCA has been extensively applied as a design-support tool for highlighting environmental criticalities and improvement solutions in the life cycle of bio-based energy systems such as H₂ (Hajjaji, 2014), bioethanol (Morales et al., 2015), biogas (Tufvesson et al., 2013), biodiesel (Castanheira et al., 2015) and second generation biofuels (Lindorfer et al., 2014).

The main objective of this study is to provide accurate conditions for sustainable H₂ production via ATR of bioethanol. Indeed, for this purpose, a comprehensive thermo-environmental study of an H₂ production system from bioethanol has been carried out based on energetic and exergetic analyses and environmental assessment.

Materials and methods

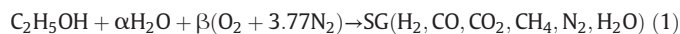
In this study, various assessment tools are simultaneously applied to investigate a H₂ production system by ATR of bioethanol. These tools are used to design and simulate the entire H₂ production process. The simulation results are used to investigate the energetic and exergetic performances and to study the environmental performance using LCA methodology. Another relevant aspect of this research is a supporting parametric investigation. The process operating parameters are varied to illustrate their influence on the system energetic, exergetic and environmental performance and to provide guidance for future research and development efforts in process design. The variation of parameters was performed using two methods: (1) the intuitive method, where the levels of all parameters except one are fixed and the response is measured for several values of the varied parameter, and (2) a factorial Design of Experiments (DOE) method. To the best of the authors' knowledge, the combination of these tools has not been considered in the past and constitutes a key aspect of this research.

Process design and simulation

Fig. 1 shows a simplified flow diagram of a conventional H₂ production process by ATR of ethanol. The process consists of a reforming section coupled to a CO clean-up section introduced to guarantee H₂ production with a CO content compatible with fuel cell specifications (Salemme et al., 2009). As described by other authors, the H₂-rich gas obtained could be directly fed to the PEMFC anode without any additional purification because all other elements present (CO₂, H₂O, etc.) could be considered as an inert admixture (Salemme et al., 2009). However, in order to produce high-purity H₂, additional purification operations are required, such as membrane separation, pressure swing adsorption (PSA), etc.

The first step of the ATR process involves reacting ethanol with steam and air to produce a synthesis gas (SG), a mixture primarily made up of H₂, CO, CO₂, CH₄, N₂ and H₂O.

The ATR reaction of ethanol can be modeled to reflect the following relationship:



where α and β are the stoichiometric coefficient of water and air (oxygen), respectively.

The main possible reactions for the ATR of ethanol are as follows:

The overall reaction of ethanol SR:



Ethanol oxidation:



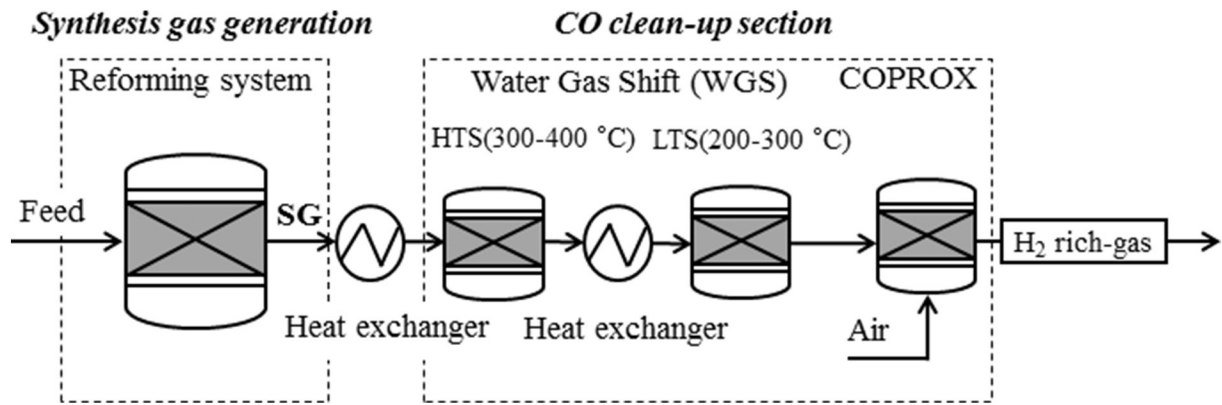
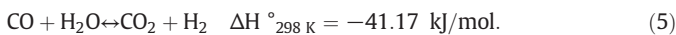
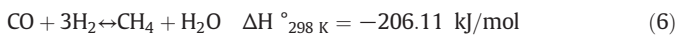


Fig. 1. A simplified flow diagram of H₂ production process.

Water gas shift (WGS):



Methanation:



Methane CO₂ reforming:



Carbon formation:



The SG composition depends on the reformer temperature (T), pressure (P), steam to ethanol molar feed ratio (SC) and oxygen to ethanol feed ratio (OC) (Rabenstein and Hacker, 2008).

As detailed below, various H₂ configurations were simulated by Aspen Plus™ software to get all required data for energetic, exergetic and environmental analyses. In all considered configurations, the pressure is kept constant at 3 bar (the operating pressure of the fuel cell) (Ersoz et al., 2006).

One of the main advantages of ATR process is its thermal self-sustaining operation. In fact, in ATR process, oxygen supplies the necessary heat via the oxidation reaction for endothermic SR; therefore, increasing the OC ratio decreases the external heat requirement (Hajjaji et al., 2014). As a result, it is possible to operate the reformer with no external energy for cooling or heating (thermoneutral condition), which makes it valuable from an energy consumption point of view (Kale and Kulkarni, 2010). In this paper, the SC ratio and reforming temperature are changed parametrically to determine their influence on system energetic, exergetic and environmental performances. However, the OC ratio

is adjusted, for each configuration, to have thermoneutral condition of the reformer. Besides, for the base case investigation the SC and temperature are considered to be 6 and 600 °C, respectively. These values are, indeed, recommended by several authors (Rabenstein and Hacker, 2008; Salemme et al., 2009) as favorable conditions for ATR of bioethanol.

The oxygen source could be either pure oxygen or air. In the present work, air was used as an oxygen carrier because using pure oxygen is not economical. Rabenstein and Hacker (2008) showed that the major products of the ATR of ethanol are water, hydrogen, methane, carbon monoxide, nitrogen, and carbon dioxide. Consequently, the component list in the SG was restricted H₂O, H₂, CH₄, CO, N₂ and CO₂. The authors showed that soot (coke) is absent at SC ratio above 3 and when temperature is above 300 °C (Rabenstein and Hacker, 2008). For this reason, carbon is excluded from the component list as plausible product since all of the considered configurations have SC > 3 and T > 300 °C.

In the second step, the SG exiting the reformer is passed through a CO cleanup section introduced to guarantee H₂ production with a CO content compatible with fuel cell specifics (levels below 10 ppm (Lei et al., 2015)). The clean-up section is made up by WGS and CO preferential oxidation reactors (COPROX) (Salemme et al., 2009). In practice, the WGS reaction takes place in two reactors: a High Temperature Shift reactor (HT-WGS), operating between 300 and 400 °C, and a Low Temperature Shift reactor (LT-WGS), operating between 200 and 300 °C (Rahimpour et al., 2012).

Because of the equilibrium constraint of the WGS reaction, the content of CO in the SG cannot be reduced to meet the desired specification for PEMFC operation. Consequently, the gas leaving the LT-WGS is mixed with air before entering the COPROX reactor, where the remaining CO is oxidized to CO₂ via Eq. (12).



In a COPROX reactor, a noble metal catalyst is employed and CO is selectively oxidized to CO₂ with trace air (Lei et al., 2015). Meanwhile, a small amount of H₂ is also oxidized to H₂O (Eq. (13)). This implies that catalyst selectivity and the precise control of the air stream are extremely important for the COPROX unit because H₂ oxidation greatly influences the system efficiency. In fact, a lack of air (oxygen) can result in the inefficient operation of the reactor because the CO concentration will not be sufficiently reduced. In contrast, an excess of air (oxygen) produces an excessive oxidation of H₂, reducing its production (Giunta et al., 2007). Thus, there is a trade-off between high and low air (oxygen)/CO ratios. In this work, the air flow rate is adjusted to obtain a molar CO concentration lower than 10 ppm with 1% of H₂ conversion.



The detailed flowsheet of the ATR process is depicted in Fig. 2.

The H₂ production process began by pumping the water-ethanol mixture. Before entering the reformer reactor, the mixture was then

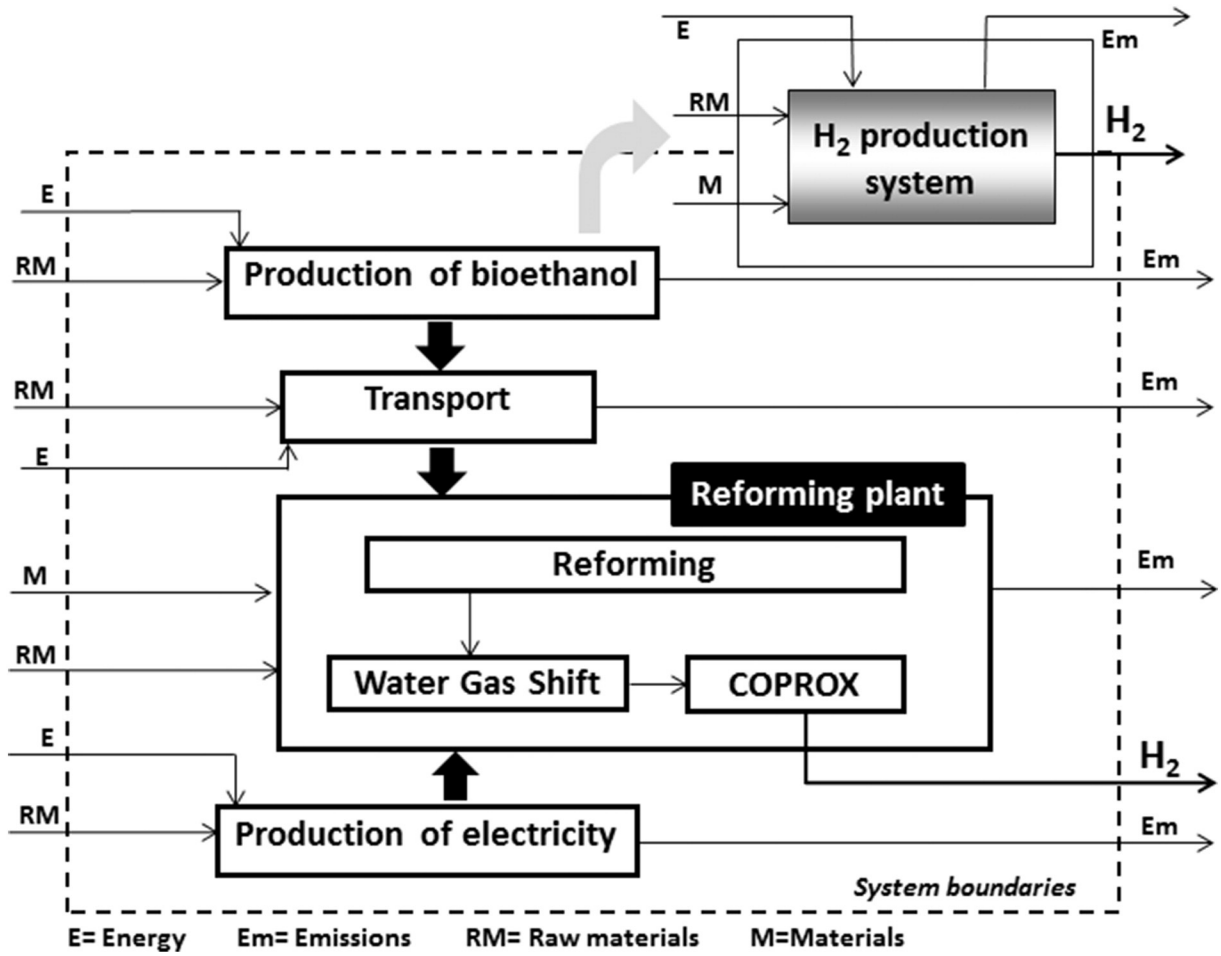


Fig. 3. Overview of the LCA boundaries of the H₂ production system.

from its initial state to the dead state by processes during which the stream may interact only with the environment. This exergy may be split into three components (physical, chemical and mixing) as shown in Eq. (17).

$$EX_M = EX_{phys} + EX_{chem} + EX_{mix}. \tag{17}$$

The physical exergy (EX_{phys}) is defined as the maximum amount of work that can be obtained when a stream of matter is taken reversibly from its initial (actual) state at P_1 and T_1 to the environmental state at

T_0 and P_0 (where thermal and mechanical equilibria exist) by physical processes. EX_{phys} is given by Eq. (18) (Hinderink et al., 1996):

$$EX_{phys} = \Delta_{\text{actual state-ref state}} \left\{ D \cdot \left(x_l \left(\sum_{i=1}^n x_i H_i^l - T_0 \sum_{i=1}^n x_i S_i^l \right) + x_v \left(\sum_{i=1}^n y_i H_i^v - T_0 \sum_{i=1}^n y_i S_i^v \right) \right) \right\} \tag{18}$$

where D is the total molar flow rate, n is the number of chemical species in the material stream, x_l and x_v are the liquid mole fraction and vapor mole

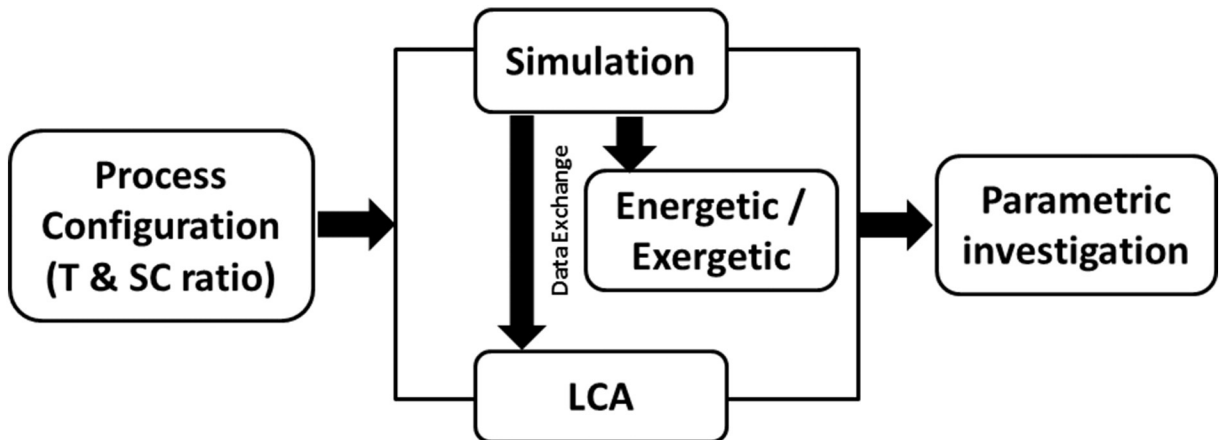


Fig. 4. Parametric investigation framework.

Table 1
Types of exergy exchanged in the process.

Exergy exchanged		
Ex _{in}	407.71	kJ/mol H ₂
Ex _{out}	294.95	kJ/mol H ₂
Ex _{destruction}	112.76	kJ/mol H ₂
Ex _{exhaust}	56.02	kJ/mol H ₂
Ex _{unused}	168.78	kJ/mol H ₂
Thermal efficiency	65.5	%
Exergy efficiency	58.6	%
Hydrogen productivity	3.42	mol H ₂ /mol ethanol

fraction, respectively, in the material stream, x_i and y_i are the mole fraction of species i in the liquid and vapor phases, respectively, and H_i and S_i are the molar enthalpy and molar entropy, respectively, of pure component i . The subscripts l and v refer to the liquid and vapor phases, respectively.

The chemical exergy is equal to the maximum amount of work obtainable when the substance under consideration is brought from the environmental state, defined by the parameters T_0 and P_0 , to the dead state by processes involving heat transfer and exchange of substances only with the environment (1987). The chemical exergy is given by Eq. (19) (Hinderink et al., 1996):

$$Ex_{chem} = D \cdot \left(x_{0,l} \sum_{i=1}^n x_{0,i} \cdot \varepsilon_{chem,i}^{ol} + x_{0,v} \sum_{i=1}^n y_{0,i} \cdot \varepsilon_{chem,i}^{ov} \right) \quad (19)$$

where $\varepsilon_{chem,i}^{ol}$ and $\varepsilon_{chem,i}^{ov}$ are the standard chemical exergy of species i in the liquid and vapor phases, respectively. The chemical exergies of the process components ($\varepsilon_{chem,i}^{ol}$ and $\varepsilon_{chem,i}^{ov}$) are evaluated using the reference environment composition as defined by Szargut et al. (1998). The environmental temperature and pressure used in this work are 298.15 K (T_0) and 1 atm (P_0), respectively.

The mixing exergy, which always has a negative value, is shown in Eq. (20) (Hinderink et al., 1996).

$$Ex_{mix} = \Delta_{mix}H - T_0 \Delta_{mix}S \text{ at}(T, P) \quad (20)$$

with

$$\Delta_{mix}M = D \cdot \left(x_l \left(M^l - \sum_{i=1}^n x_i M_i^l \right) + x_v \left(M^v - \sum_{i=1}^n y_i M_i^v \right) \right) \quad (21)$$

where M is any thermodynamic property.

The superscripts l and v denote the thermodynamic property of the mixture in the liquid or vapor phase, respectively.

The exergy destroyed within the bioethanol reforming process may be calculated by two methods. The first calculation method is global and consists of determining the form of the exergy and performing an exergy balance for the entire reforming process using Eq. (22). The exergy destruction is written as

$$Ex_{destruction} = Ex_{in} - Ex_{out} \quad (22)$$

with

$$Ex_{in} = Ex_{flow 1} + Ex_{flow 7} + Ex_{flow 17} + W_{Compressor 1} + W_{Compressor 2} + W_{Pump} \quad (23)$$

and

$$Ex_{out} = Ex_{flow 16}. \quad (24)$$

The exergy of the hydrogen-rich gas (flow 16) can be assumed to be the sum of the exergy of pure H₂ and the exergy of the wasted gas.

$$Ex_{flow 16} = Ex_{H_2} + Ex_{Wasted-gas}. \quad (25)$$

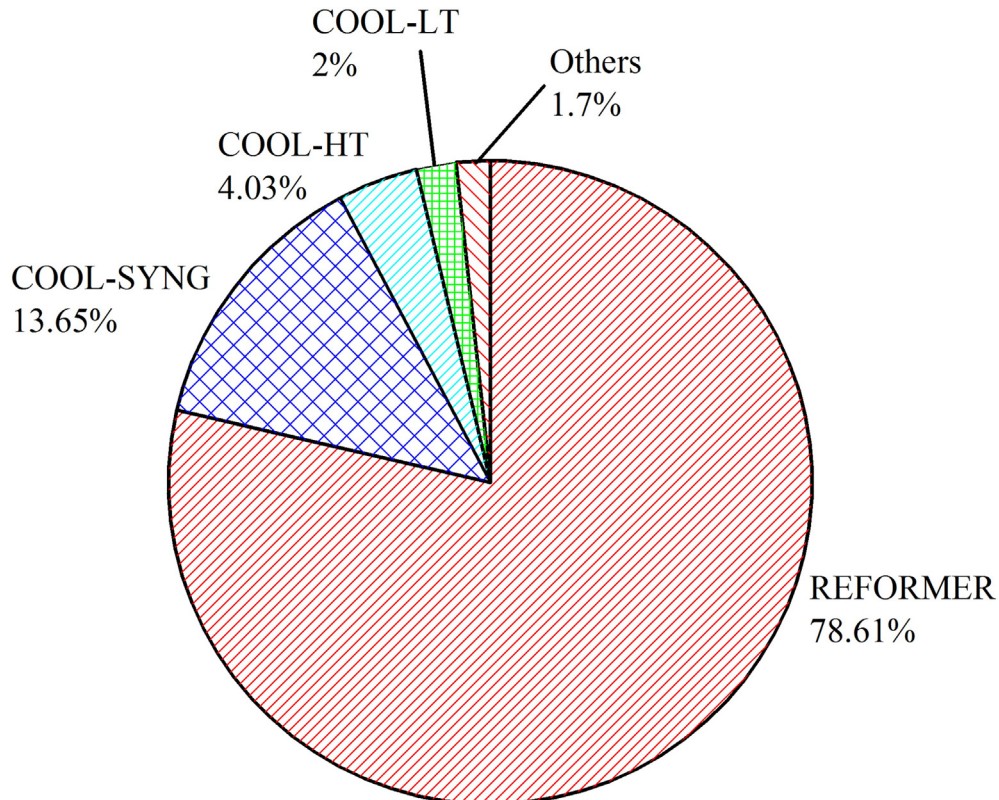


Fig. 5. Process exergy destruction breakdown.

Table 2
Main inventory data for the production of hydrogen (1 kg).

	Value	Unit
Input		
Materials		
Ethanol	6.73	kg
Water	15.80	kg
Energy		
Electric energy	776.64	kJ
Transport by trucks	0.67	t.km
Outputs		
Products		
H ₂	1	kg
Emissions		
CO ₂	11.99	kg
H ₂ O	13.97	kg
CH ₄	0.032	kg
CO	0.00	kg

The unused exergy is given by Eq. (26):

$$EX_{\text{unused}} = EX_{\text{destruction}} + EX_{\text{Wasted-gas}}. \quad (26)$$

The exergetic efficiency of the system is given by Eq. (27)

$$\eta_{\text{Exergy}} = \frac{EX_{H_2}}{EX_{\text{in}}} = 1 - \frac{EX_{\text{unused}}}{EX_{\text{in}}}. \quad (27)$$

To pinpoint the location and magnitude of primary exergy destruction and thus showing the direction for improvements, the detailed method is applied. The first method (global) is rapid and gives no indication of the distribution of the destroyed exergy, whereas the detailed method provides the contribution of each component on the thermodynamic imperfection of the process (the destroyed exergy).

$$EX_{\text{destruction}} = \sum_i EX_{\text{destruction},i} \quad (28)$$

with

$$EX_{\text{Destruction},i} = \sum_i EX_{\text{in},i} - \sum_i EX_{\text{out},i}. \quad (29)$$

Life cycle assessment

The objective of this part is to assess the environmental impacts associated with the production of H₂ from ATR of bioethanol using the LCA methodology. The LCA reported here is coherent with ISO 14040–14,044 standards which includes four interrelated phases: (1) goal and scope definition, (2) life cycle inventory (LCI), (3) life cycle impact assessment (LCIA), and (4) interpretation (2006). SimaPro 8 software (Goedkoop et al., 2013) has been used to perform the

assessment, whereas the Ecoinvent default database v3.1 (Ecoinvent, 2013) has been employed to calculate the life cycle inventory.

Goal and scope definition

Goal and scope. The main objective of this study is to evaluate the life-cycle environmental burdens of an H₂ production system based on ATR of bioethanol and to identify the environmental hot spots (the elements that have a high contribution to the environmental burden). In order to perform the parametric investigation, LCA studies have been achieved for each process configuration as described below.

Functional unit, system boundaries, and common assumptions. The functional unit (FU) chosen in this study is one kg of H₂ produced from ATR of bioethanol. The system function was set as the production of H₂ at the gate of the plant. Use and end-of-life of the product were not included. All emissions, materials and energy consumption and transport are based on this FU.

The system boundaries (SB), depicted in Fig. 3, encompasses all the processes necessary to deliver the system's FU. The SB included four main subsystems: (1) bioethanol production, (2) transport of bioethanol, (3) reforming process and (4) production of electricity required by the reforming process.

Bioethanol production data are provided by Ecoinvent v3. It is modeled as ethanol, 95% in H₂O, from sugar beet molasses, at distillery/CH S. This process was chosen after the analysis of different scenarios for bioethanol in Ecoinvent v3 database. Bioethanol derived from sugar beet molasses seems to best describe the Tunisian context. In Tunisia, sugar has mainly been produced from beets with a rate of 30,000 tons per year (2015b). Assuming that for each ton of sugar 0.5 ton of molasses is coproduced (2015a), it follows that approximately 15,000 tons of sugar beet molasses were generated in Tunisia in 2013. This amount could be used as a renewable feedstock for bioethanol production. The transportation implies the transport of bioethanol to the reforming unit. The transportation is performed by lorry modeled in SimaPro database as "Lorry 16-32 metric ton-EURO5 market" (Ecoinvent, 2013). This study assumed an average transportation distance of 100 km. The H₂ production process considered here uses electricity purchased from the grid to operate the process components (compressor, pump, etc.). Nevertheless, the production of electricity consumes resources and releases pollutants into the atmosphere. Therefore, a subsystem "Electricity production" was considered to pinpoint the contribution of electrical energy generation to the environmental impacts of the entire H₂ system. However, to reproduce the Tunisian electricity mix (97% from natural gas and 3% hydroelectricity), which is not included in the SimaPro databank, the electricity production is supposed to be only by gas. It is worth mentioning that the construction and decommissioning phases and the manufacture and recycling of reforming catalysts are not considered in this study.

Table 3
Characterization results for 1 kg of H₂.

Impact category	Total	Reforming plant	Prod. bioethanol	Transport	Prod. electricity
ADP (kg Sb eq)	4.87E-02	2.37E-06	1.98E-02	8.27E-04	2.81E-02
AP (kg SO ₂ eq)	2.76E-02	1.94E-06	8.68E-03	3.91E-04	1.85E-02
EP (kg PO ₄ ³⁻ eq)	2.81E-02	7.99E-07	9.55E-03	8.87E-05	1.84E-02
GWP (kg CO ₂ eq)	7.27	0.64	2.77	0.11	3.74
ODP (kg CFC-11 eq)	3.13E-06	5.16E-11	3.56E-07	2.08E-08	2.75E-06
HTTP (kg 1.4-DB eq)	5.14E-01	8.51E-05	8.08E-02	6.50E-03	4.26E-01
FAETP (kg 1.4-DB eq)	1.80	4.56E-04	4.25E-01	1.49E-02	1.36
MAETP (kg 1.4-DB eq)	2.99E-01	4.52E-05	7.42E-02	2.41E-03	2.22E-01
TEP (kg 1.4-DB eq)	2.59E-02	2.45E-06	6.46E-03	2.50E-04	1.92E-02
POFP (kg C ₂ H ₄ eq)	1.65E-03	1.92E-04	5.54E-04	1.95E-05	8.89E-04

Life cycle inventory (LCI) analysis

LCI involves the collection and computation of data to quantify relevant inputs and outputs associated with the production of the FU. As described above, the reforming plant was simulated in Aspen Plus™ to provide foreground inventory data for the LCA of the H₂ production system. The background LCI data (e.g., LCI of 1 kWh electricity, 1 kg of bioethanol, etc.) was provided by the Ecoinvent database v3 (Ecoinvent, 2013).

Life cycle impact assessment (LCIA)

LCI data were computationally implemented into SimaPro 7.3 (Goedkoop et al., 2013) to carry out the LCIA.

To achieve the goal and the scope of this study two impact assessment methods are used: CML baseline 2000 method (Guinée et al., 2002) and ReCiPe method (Goedkoop et al., 2012). The midpoint-based CML baseline 2000 method is commonly used in most H₂ LCA studies. Moreover, the choice of this method enables the comparison of our system with other published H₂ production alternatives (comparison at similar impact evaluation method). Seven environmental impact categories were quantified: global warming potential (GWP), abiotic depletion potential (ADP), eutrophication potential (EP), acidification potential (AP), ozone layer depletion potential (ODP), photochemical oxidant formation (POFP), and human toxicity potential (HTP). The second method “ReCiPe” provides an endpoint single score used in the parametric investigation.

Parametric investigation

The main motivation of this section is to examine the influence that the reformer operating temperature and SC ratio have on energetic, exergetic and environmental performances of the system. To provide a comprehensive understanding, two methods are applied: (1) the intuitive method and (2) the DOE method. Fig. 4 presents the parametric investigation framework.

Intuitive method

The intuitive method varies one operating parameter (T or SC ratio) while holding the other constant at its base-case value. The base values are T = 600 °C and SC = 6.

Design of the experimental method

In contrast to the intuitive method, the DOE method examines the simultaneous influence of the reformer temperature and the S/C ratio on the process energetic, exergetic and environmental performances. The DOE method gives more information per experiment than the unplanned approaches (intuitive method), allows us to see the interactions among experimental variables within the range studied, leads to better knowledge of the process and therefore reduces research time and costs. The main outcome of this DOE method is the development of mathematical models that predict how changes in the reformer operating parameters (T and SC ratio) affect the performances (energetic, exergetic and environmental).

In the two-level factorial experiment methodology, each factor (variable) (Z_i) is characterized by two different levels (the minimum, Z_i^{\min} , and the maximum, Z_i^{\max}) (Kafarov, 1974). For statistical calculations the actual values of variables were scaled up (coded) according to Eq. (30).

$$x_i = (Z_i - Z_i^0) / \Delta Z_i \quad (30)$$

where

$$\Delta Z_i = (Z_i^{\max} - Z_i^{\min}) / 2 \quad (31)$$

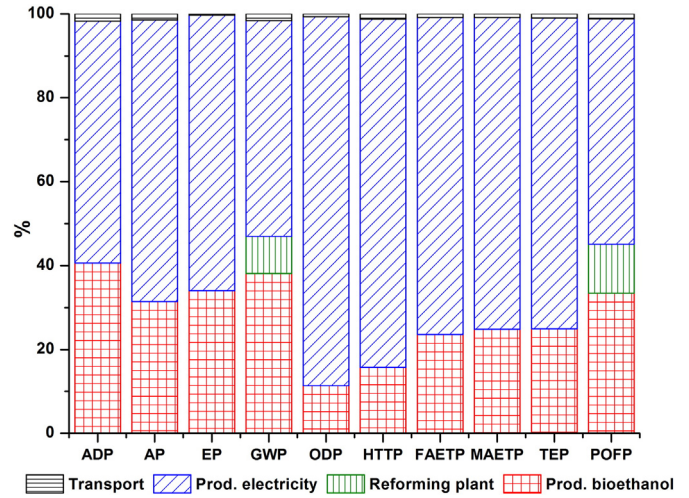


Fig. 6. Relative contribution of each subsystem to the environmental impacts of the ATR of bioethanol system.

and

$$Z_i^0 = (Z_i^{\max} + Z_i^{\min}) / 2 \quad (32)$$

where Z denotes the actual value of design variable, Z^0 the center point of design variable, ΔZ the interval of variation and x the coded level of design variable (a dimensionless value). Basically, the extent of each variable involves three different coded levels from low (−1) to medium (0) to high (+1).

Generally, most factorial experiments are developed on the basis of two-level factors with a linear relationship between the parameters for simplicity. However, according to the intuitive method results, the factors appear to have a non-linear relationship with the energetic and exergetic efficiencies. Therefore, a central composite design (CCD) of orthogonal type was employed in this study. The axial level (“star point”) β has been computed from the condition for a CCD to be an orthogonal design as described by the references (Kafarov, 1974). For two independent variables (SC ratio and T), the value of the star point is $\beta = 1$ (Kafarov, 1974).

The corresponding response surface model (RS model), known also as a regression or an empirical equation, represents a second-order polynomial approximation of experimental data and is stated by the

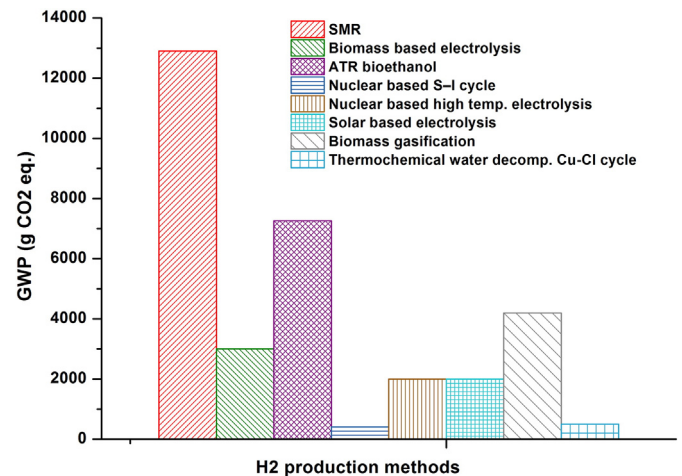


Fig. 7. Relative comparison of the GWP impact of the ATR of bioethanol system and other alternative routes for H₂ production.

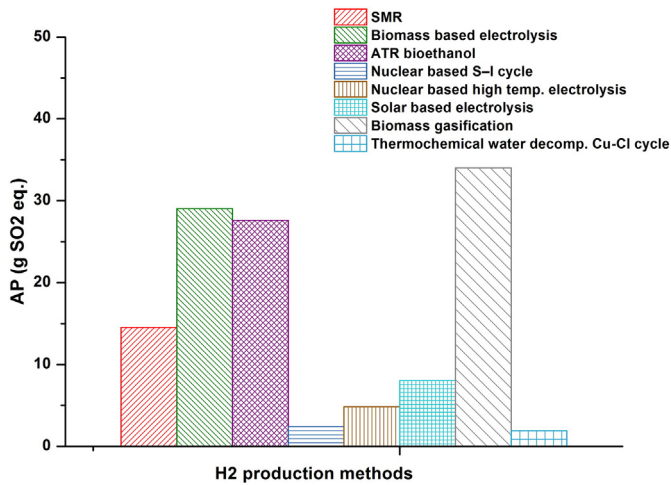


Fig. 8. The relative comparison of the AP impact of the ATR of bioethanol system and other alternative routes for H₂ production.

following relationship (Eq. (33)) (Poroch-Seritan et al., 2011):

$$Y = a_0 + a_1x_1 + a_2x_2 + a_{12}x_1x_2 + a_{11}x_1^2 + a_{22}x_2^2 \quad (33)$$

where Y is the predicted response (thermal or exergy efficiency) caused by the parameter variation, a_i is the regression coefficient, and x_1 and x_2 are the coded variables for the SC and T, respectively. The term $(a_1x_1 + a_2x_2)$ represents the linear effect of each individual parameter, and the term $(a_{12}x_1x_2)$ characterizes the interactions between parameters x_1 and x_2 . The non-linear behavior of each parameter is presented in the quadratic terms $(a_{11}x_1^2 + a_{22}x_2^2)$.

The number of experiments required to establish this model, via the CCD method, is $N = 2^k + 2k + 1$, where k is the number of independent variables. For $k = 2$, $N = 9$, and 9 experiments are required. The regression coefficients of the mathematical model are determined independently by Eq. (34) (Kafarov, 1974):

$$a_j = \frac{\sum_{i=1}^N x_{ji}y_i}{\sum_{i=1}^N x_{ji}^2} \quad (34)$$

where x_{ji} is the value of the element corresponding to the j th column and the i th line of the second-order orthogonal matrix.

The conditions of the i th study (experiment) are given by line “i” in the DOE matrix. The result of study “i” provides the i th element of the vector response Y, namely y_i . Depending on the case of study, the response y_i may be the process thermal efficiency, the exergetic efficiency

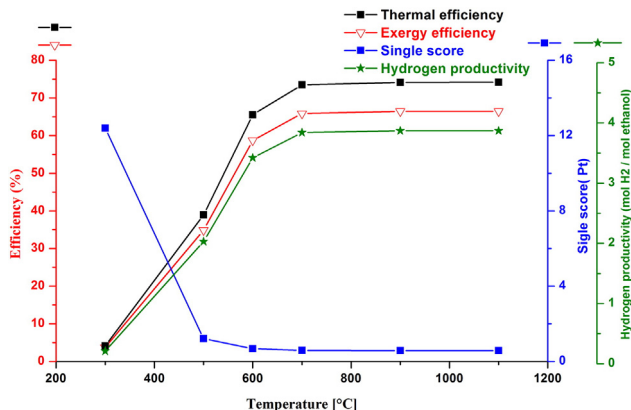


Fig. 9. The influence of the reformer operating temperature on the system efficiencies.

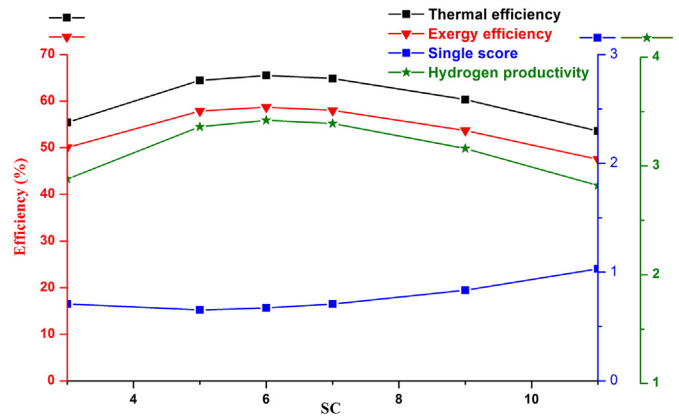


Fig. 10. The influence of the SC ratio on the system efficiencies.

or the process single score (provided by ReCiPe method). Each response y_i is computed by applying the following series of steps: (1) simulation of the SR process with the corresponding reformer parameters given by line “i” of the design matrix, (2) calculation of the process thermal and exergetic efficiencies (determination of the process stream exergy (Ex_{in} , Ex_{out} , $Ex_{destruction}$, etc.)) and (3) performing LCA (process single score).

Results and interpretation

Process design and simulation

The simulation of the ATR of bioethanol provides the properties of the stream (T, P, molar flow, stream composition, etc.) at different locations. The stream properties of the base case process can be found in Table A.1 in the Supplementary material.

Energy and exergy analyses

The thermal efficiency of the ATR process, computed by Eq. (14), is 65.5%. The efficiency value indicates that about two-thirds of the energy fed to the ATR process is recovered as the useful product (H₂) and that the remaining part of incoming process energy is vented to the atmosphere (exhausted). It can be noticed that the thermal efficiency of the ATR process is relatively lower than those reported in literature and relative to other reformates (methane: 81.4% (Wang, 2008), propane: 84.2 (Liu et al., 2006) and gasoline: 82–84% (Danial Doss et al., 2001)).

The stream exergy of the process (described by Eqs. (12)–(16)) is provided in Table A.2 in the Supplementary material. The different forms of the exergy exchanged in the process (computed according to Eqs. (22)–(26)) are summarized in Table 1.

The exergetic efficiency of the ATR process (described by Eq. (27)) is 58.6%. This efficiency is about 7% less than the process thermal efficiency. This difference occurs because the exergetic efficiency includes a term for the exergy that is exhausted (in the wasted gas, given by Eq. (25)) and a term for the exergy that is destroyed. The latter exergy ($Ex_{destruction}$, given by (Eq. (22)) is not taken into account by the first law of thermodynamics when calculating the process thermal efficiency. About 41.4% of the overall exergy provided to the plant is unused.

Table 4
Levels of process variables in actual values and coded units.

	SC	T [°C]
Z_i^{\min}	3	300
Z_i^{\max}	9	900
Z_i^0	6	600
ΔZ_i	3	300
x_i	(SC-6)/3	(T-600)/300

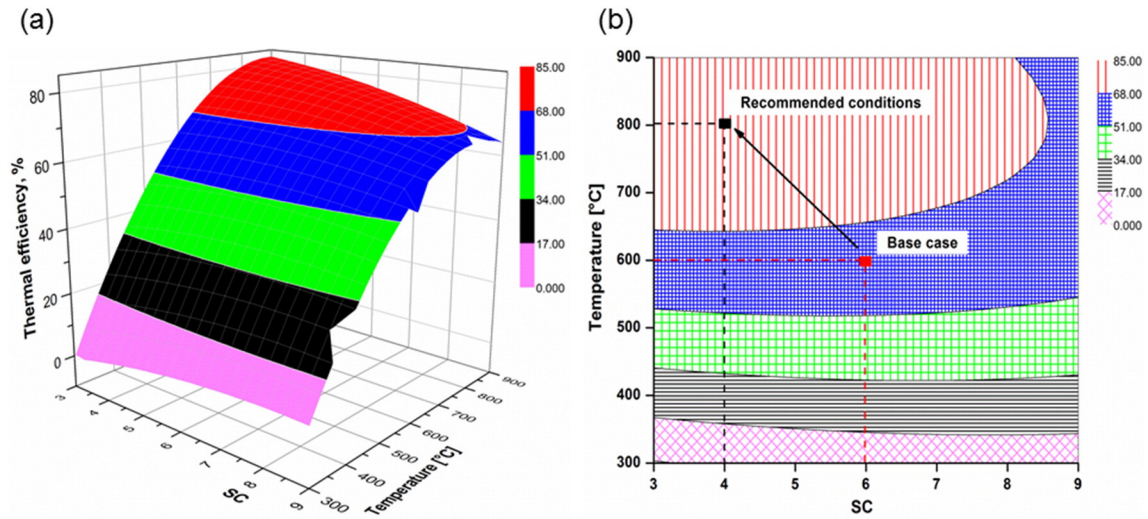


Fig. 11. The influence of the reformer temperature and SC ratio on the process thermal efficiency (a) response surfaces plot and (b) contour-surfaces map.

About two-thirds of this unused exergy vanishes as exergy destruction within the individual components of the process.

Fig. 5 graphically displays the contribution of the process component to the destroyed exergy. As clearly demonstrated in this figure, greater exergy destruction occurred in the reformer (78.6%) due to the high irreversibility of the chemical reactions (Iribarren et al., 2014). This means that this component should have the highest priority for process improvement from the thermodynamic point of view. COOL-SYNG comes in the second position in terms of the destroyed exergy with a contribution of 13.7% followed by COOL-HT (4%). Only 3.7% of the total exergy destruction of the process occurred in other plant components.

Table 1 shows that the production of 1 mol of H₂ induces the destruction of 112.76 kJ (approximately 28% of the exergy entering the ATR process) owing to the irreversibility of thermodynamic transformations. This value remains comparatively higher than that reported in the literature for SMR (100.68 kJ/mol H₂) (Simpson and Lutz, 2007) and ATR of glycerol (98.82 kJ/mol H₂) (Hajjaji et al., 2014).

Life cycle assessment

The main inventory data of the ATR process for 1 kg of H₂ are summarized in Table 2. Table 3 gathers the environmental characterization

results evaluated according to the CML 2000 method. In order to highlight the processes with the highest environment impact on the life-cycle performance of the system, the contributions to the individual impact are broken down in Fig. 6 and discussed in detail below.

In Fig. 6, the results show that for the production of electricity contributes to the highest in each category of environmental impact considered. Therefore, electricity consumption is the main hotspot within the whole H₂ production system and should have, therefore, the highest priority for process improvement from environment point of view. Five impact categories are detailed in this interpretation section: GWP, ADP, AP and EP. These are among the most common and well-established impact categories for assessing bioenergy systems in LCA studies (Cherubini and Strømman, 2011; Muench and Guenther, 2013; Peters et al., 2015).

The total GHG emissions of the system are estimated to be approximately 7.26 kg CO₂-eq per kg of H₂ produced. Approximately 51% of these emissions are attributed to the production of electricity consumed during the reforming process. The production of bioethanol subsystem contributes about 38% to the GWP impact. This, especially due to the large amount of heat from fuel combustion consumed during bioethanol production in distillation, drying, etc., as well as to the emission of NO_x associated with the use of fertilizers during beet production. The reforming plant contributes by only 8.8% to the GWP impact.

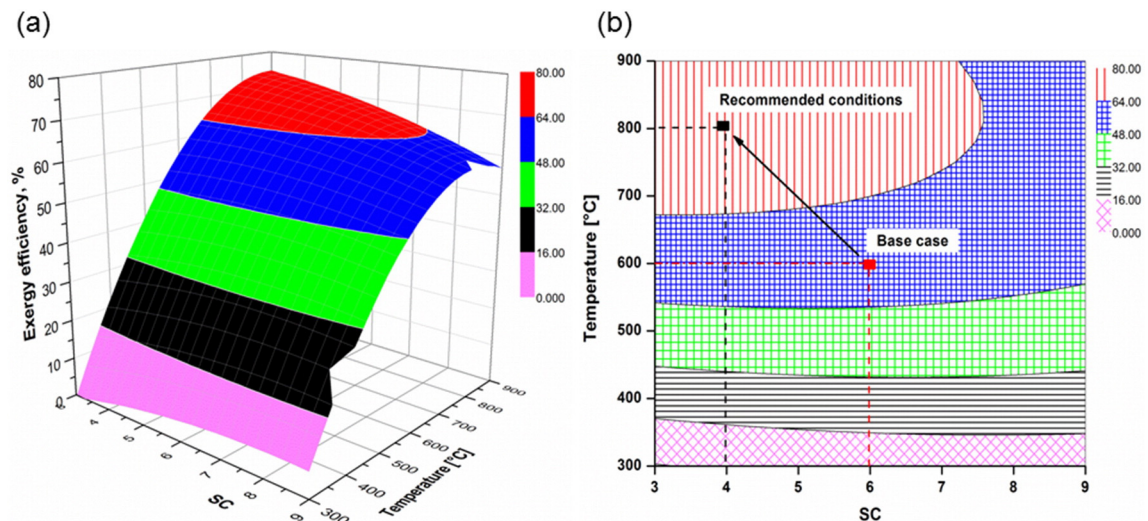


Fig. 12. The influence of the reformer temperature and SC ratio on the process exergy efficiency (a) response surfaces plot and (b) contour-surfaces map.

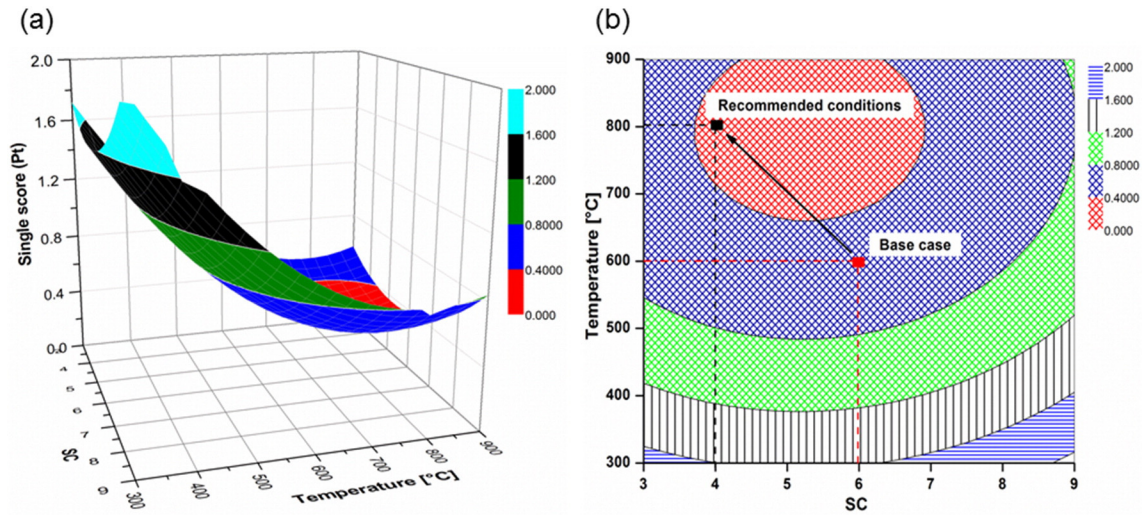


Fig. 13. The influence of the reformer temperature and SC ratio on the system single score (a) response surfaces plot and (b) contour-surfaces map.

The result of the GWP impact of the H_2 production system is compared with previously conducted studies (Ozbilen et al., 2011) and is given in Fig. 7. As observed in this figure, the lowest emission values belong to bio-based H_2 production methods. The ATR of bioethanol system is found to emit about half of the life cycle GHG of a conventional H_2 production system (SMR). This could be highlighted as an environmental advantage. Nevertheless, this impact category could be further improved by a rational choice of the reforming process operating conditions (T and SC ratio).

The AP impact category is mainly associated with the emission of nitrogen oxides (NO_x) and sulfur oxides (SO_x) during the production of H_2 . The acidifying pollutants of the ATR of bioethanol system are estimated to be approximately 0.027 kg SO_2 -eq per kg of H_2 . About two third of these emissions are generated during the production of electricity subsystem. This is primarily due to the high sulfur content in the fuel (natural gas) used for electricity generation. Bioethanol production subsystem has a significant contribution to the AP impact (~31%). That is a consequence of the large emissions of NO_x and SO_x during (i) the agricultural phase for sugar beet production mainly due to the use of ammonia as a fertilizer (ii) the combustion of sulfur-containing fossil fuels during bioethanol production in distillation, drying, etc.

In Fig. 8 we graphically compare the AP impact for H_2 production processes stated above (GWP interpretation) (Ozbilen et al., 2011). The AP impact of bioethanol-to- H_2 system remains, however, greater than the AP of the other considered alternatives.

The ADP impact is dominated by the production of electricity (~58%), which consumes significant amounts of nonrenewable fuel. The production of bioethanol contributes approximately 41% to the

ADP impact. This is related to the intensive use of energy fossil fuel and phosphate ore for the production of the mineral fertilizer used during beet production. EP impact category represents the eutrophication contribution to ecosystems like lakes and river. In total, EP impact is estimated to be approximately 0.028 kg PO_4^{3-} -eq per kg of H_2 . The main source of the EP impact comes from the electricity production subsystem (~66%) followed by bioethanol production (~34%).

Parametric investigation

Intuitive method

Fig. 9 shows the effects of reforming temperature on process efficiencies (energetic, exergetic and environmental). The temperature has a significant influence on energetic performances. With the increase in the reforming temperature from 300 to 700 °C, the energetic and the exergetic efficiencies increased from approximately 3% to 65%, until they reached a maximum plateau at approximately 70%, after which they remained constant. This behavior can be explained through an evaluation of the H_2 production of the ATR process. In fact, the H_2 yield was found to increase with an increase in the reforming temperature, reaching a maximum and then decreasing slightly as observed in Fig. 9. This is because the overall reaction of ethanol SR (Eq. (2)) is endothermic, and a higher reforming temperature shifts the equilibrium position towards the product side resulting in an increased H_2 production. The increase in H_2 yield increases the system efficiencies (energetic and exergetic). However, WGS (Eq. (5)) and methanation (Eqs. (6) and (7)) reactions on the other hand are exothermic in nature and the equilibrium shifts towards the reactant side with an increase in the reforming temperature resulting in consumption of H_2 produced during the SR reaction. The competition between the SR reaction and the WGS and methanation reactions makes plateaus in H_2 productivity, in thermal efficiency and in exergy efficiency at approximately 700 °C. However, the process single score has a relatively different behavior. It has been shown above (the LCA interpretation) that the electricity consumption and bioethanol production subsystems are the most significant environmental steps from this point of view. Accordingly, the best alternative is the one that consumes minimum electrical energy (maximum thermal efficiency) and uses less bioethanol for the production of a given amount of H_2 (this is the inverse of H_2 productivity). In other words, the alternative consuming more bioethanol (low H_2 productivity) and electrical energy has the poorer environmental performance (high single score). It is thus clear that the single score varies inversely as H_2 productivity and these two proprieties reach plateaus simultaneously.

Fig. 10 shows that the SC ratio has no significant effect on the energetic and exergetic efficiencies. These efficiencies increase slightly and

Table 5

The main results from investigating the ATR process at the recommended conditions.

Exergy exchanged	Value	Unit
EX_{in}	326.74	kJ/mol H_2
EX_{out}	256.62	kJ/mol H_2
$EX_{destruction}$	70.12	kJ/mol H_2
$EX_{exhaust}$	14.97	kJ/mol H_2
EX_{unused}	85.09	kJ/mol H_2
Thermal efficiency	82.18	%
Exergy efficiency	73.96	%
Hydrogen productivity	4.27	mol H_2 /mol ethanol
Single score	0.391	Pt
Characterization results		
ADP	8.66E-06	kg Sb eq
AP	1.72E-02	kg SO_2 eq
EP	1.79E-02	kg PO_4^{3-} eq
GWP	4.36	kg CO_2 eq

then decrease. Again, this behavior can be explained by the evolution of H₂ productivity. In fact, with an increase in the SC ratio, the number of moles of water on the reactant side of Eqs. (2) and (5) increases and hence the equilibrium of SR and WGS shifts towards the product side resulting in increased H₂ yield. Unfortunately, this excess water decreases the energetic and exergetic process efficiencies. As the SC increases, the heat requirement for heating and vaporizing the feed (stream 2 → stream 6 (in Fig. 2)) increases, as does the heat required for the reforming reactions (Eq. (2)), and the OC ratio increases. The additional oxygen (increase of OC) shifts the incomplete oxidation of the synthesis gas to a combustion reaction, resulting in decreased H₂ yield. In other words, the increase of OC ratio (caused by increasing the heat requirement of the process) attenuates the increase in the H₂ production that was induced by the increase of SC ratio. This observation results in small change in the H₂ productivity, thermal efficiency and exergetic efficiency. As described above, the environmental performance of the system (described by the single score) depends on H₂ productivity and energetic performance. Fig. 10 shows that the single score and H₂ productivity reach plateaus simultaneously.

Design of the experimental method

The levels of variables in real values and coded units are shown in Table 4. The DOE matrix and the second-order orthogonalized matrix can be found in the Appendix in Tables A.3 and A.4, respectively.

The second-order models with coded units obtained for the process thermal, exergy and single score are given by Eqs. (35), (36) and (37), respectively.

$$\eta_{\text{Thermal}} = 62.19 - 2.68x_1 + 35.07x_2 - 2.61x_1^2 - 21.38x_2^2 - 6.71x_1x_2 \quad (35)$$

$$\eta_{\text{Exergy}} = 55.71 - 2.68x_1 + 31.46x_2 - 2.31x_1^2 - 19.13x_2^2 - 6.23x_1x_2 \quad (36)$$

$$SS = 0.52 + 0.16x_1 - 0.60x_2 + 0.32x_1^2 + 0.46x_2^2 - 0.02x_1x_2. \quad (37)$$

These second-order models can rapidly estimate the process performances (energetic, exergetic and environmental) based on the SC ratio and temperature. To increase our understanding of the system behavior, the three models are plotted in Figs. 11–13. The interpretation of these plots is very similar to the interpretation of the intuitive method results. The increase in the SC ratio (the horizontal displacement on the contour-surfaces maps) does not affect the performance of the three processes (the same color shows levels in the same range of performance). However, the increase in the temperature increases the system performance (moves from one range to another). Moreover, it is clear from the response surface plot that at high temperature (>700 °C) the system performances reach plateaus. Beyond this value, the gain in performance is not significant when the system is under a high-temperature technological constraint.

To conclude the discussion section, it is clear that the process, when operating under conditions recommended by simple chemical reaction investigation, suffers from low performance. This is because energetic, exergetic and environmental performances are comparatively lower than similar findings previously reported by other researchers for other reformates. Moreover, the energetic optimization of a process should not be done away with at the expense of environmental optimization. Indeed, a process can have good energy performance when one or more of its raw materials pollute the environment. Considering all the above-mentioned interpretations, we recommend SC = 4 and T = 800 °C as appropriate conditions for H₂ production from ATR of bioethanol. This configuration was thoroughly investigated, and Table 5 summarizes the main results obtained. Such conditions ensure not only the lowest consumption of energy to generate a given amount of H₂ but also the best environmental performance of the entire system.

Conclusion

The present research addresses a thermo-environmental life cycle assessment of H₂ production system from bioethanol autothermal reforming. Various assessment tools are simultaneously applied. These tools imply entire H₂ production process design and simulation, energetic, exergetic and environmental studies and parametric (intuitive and design of experiment based method) analysis.

The main findings of this research can be summarized in these points:

- The thermal efficiency of the base case ATR process indicates that about two-thirds of the energy fed to the process is recovered as the useful product (H₂) and that the remaining part of incoming process energy is vented to the atmosphere.
- The exergetic efficiency of the base case ATR process is 58.6% and greater exergy destruction occurred in the reforming reactor (78.6%).
- The production of electricity (required by the reforming process) contributes to the highest in each category of environmental impact considered.
- The base case process suffers from low performance. This is because energetic, exergetic and environmental performances are comparatively lower than similar findings previously reported by other researchers for other reformates.
- The parametric study indicates that the process performances (energetic, exergetic and environmental) could be ensured by proper and rational combination of SC ratio and reforming temperature.
- Based on parametric investigation SC = 4 and T = 800 °C seems to be more accurate parameters for entire bioethanol-to-hydrogen process. Compared with the base case process, the recommended configuration has the best performances. The thermal efficiency, the exergetic efficiency and the process single score pass from 65.5% to 82.18%, 58.6% to 73.96% and 0.670 to 0.391, respectively.

Appendix A. Supplementary data

Supplementary data to this article can be found online at <http://dx.doi.org/10.1016/j.esd.2016.12.003>.

References

- Abánades A, Rubbia C, Salmieri D. Thermal cracking of methane into hydrogen for a CO₂-free utilization of natural gas. *Int J Hydrogen Energy* 2013;8491–6.
- Ahmed S, Krumpelt M. Hydrogen from hydrocarbon fuels for fuel cells. *Int J Hydrogen Energy* 2001;26(4):291–301.
- Aspen Plus™. Physical property methods and models software version [USA, Burlington, MA: USA, Burlington, MA]; 1988.
- Castanheira ÉG, Grisoli R, Coelho S, Anderi da Silva G, Freire F. Life-cycle assessment of soybean-based biodiesel in Europe: comparing grain, oil and biodiesel import from Brazil. *J Clean Prod* 2015;102:188–201. [Apr [cited 2015 May 9]; Available from: <http://www.sciencedirect.com/science/article/pii/S0959652615003972>].
- Cherubini F, Strømman AH. Life cycle assessment of bioenergy systems: state of the art and future challenges. *Bioresour Technol* 2011;102(2):437–51. [Jan [cited 2015 Jan 10]; Available from: <http://www.sciencedirect.com/science/article/pii/S096085241001360X>].
- Daniel Doss E, Kumar R, Ahluwalia RK, Krumpelt M. Fuel processors for automotive fuel cell systems: a parametric analysis. *J Power Sources* 2001;102(1–2):1–15. [Dec. Available from: <http://linkinghub.elsevier.com/retrieve/pii/S0378775301007844>].
- Divins NJ, López E, Rodríguez Á, Vega D, Llorca J. Bio-ethanol steam reforming and autothermal reforming in 3-µm channels coated with RhPd/CeO₂ for hydrogen generation. *Chem Eng Process Process Intensif* 2013;64:31–7. [Feb [cited 2015 Aug 25]; Available from: <http://www.sciencedirect.com/science/article/pii/S025527011200222X>].
- Ecoinvent. Ecoinvent database v3. Swiss Centre for life cycle inventories; 2013.
- Ersoz A, Olgun H, Ozdogan S. Reforming options for hydrogen production from fossil fuels for PEM fuel cells. *J Power Sources* 2006;154(1):67–73. [Mar [cited 2015 Aug 25]; Available from: <http://www.sciencedirect.com/science/article/pii/S0378775305006105>].
- Giunta P, Mosquera C, Amadeo N, Laborde M. Simulation of a hydrogen production and purification system for a PEM fuel-cell using bioethanol as raw material. *J Power Sources* 2007;164(1):336–43.
- Goedkoop M, Heijungs R, Huijbregts M, De Schryver AM, Struijs J, van Zelm R. ReCiPe 2008: a life cycle impact assessment method which comprises harmonised category indicators at the midpoint and the endpoint level [internet]. Report I: characterisation 1st ed.; 2012. [cited 2015 Jun 1]. Available from: <http://www.lcia-recipe.net>.

- Goedkoop M, Oele M, Leijting J, Ponsioen T, Meijer E. PRé consultants. Introduction to LCA with SimaPro [internet]. Available from: www.pre.nl, 2013.
- Guinée JB, Gorrié M, Heijungs R, Huppes G, Kleijn R, de Koning A, et al. Life cycle assessment. An operational guide to the ISO standards; 2002.
- Hajjaji N. Thermodynamic investigation and environment impact assessment of hydrogen production from steam reforming of poultry tallow. *Energ Convers Manage* 2014;79:171–9. [Available from: <http://www.sciencedirect.com/science/article/pii/S0360319907002479>].
- Hajjaji N, Baccar I, Pons M-N. Energy and exergy analysis as tools for optimization of hydrogen production by glycerol autothermal reforming. *Renew Energy* 2014;71:368–80. [Available from: <http://www.sciencedirect.com/science/article/pii/S0960148114003176>].
- Hinderink AP, Kerkhof FPJM, Lie ABK, De Swaan AJ, Van Der Kooij HJ. Exergy analysis with a flowsheeting simulator - I. Theory: calculating exergies of material streams. *Chem Eng Sci* 1996;51(20):4693–700.
- Hou T, Zhang S, Chen Y, Wang D, Cai W. Hydrogen production from ethanol reforming: catalysts and reaction mechanism. *Renew Sustain Energy Rev* 2015;44:132–48. [Apr [cited 2015 Jan 10]; Available from: <http://www.sciencedirect.com/science/article/pii/S1364032114010752>].
- Iribarren D, Susmozas A, Petrakopoulou F, Dufour J. Environmental and exergetic evaluation of hydrogen production via lignocellulosic biomass gasification. *J Clean Prod* 2014;69:165–75. [Apr, Available from: <http://linkinghub.elsevier.com/retrieve/pii/S0959652614000900>].
- Kafarov V. Cybernetic methods and chemical technology. Mosco: Mir; 1974.
- Kale GR, Kulkarni BD. Thermodynamic analysis of dry autothermal reforming of glycerol. *Fuel Process Technol* 2010;91(5):520–30.
- Karellas S, Braimakis K. Energy–exergy analysis and economic investigation of a cogeneration and trigeneration ORC–VCC hybrid system utilizing biomass fuel and solar power. *Energ Convers Manage* 2015. [Available from: <http://linkinghub.elsevier.com/retrieve/pii/S0196890415006421>].
- Lee JY, Kim YS. Optimization the process variables for the fractionation of Saccharina japonica to enhance glucan content. *J Ind Eng Chem* 2013;19(3):938–43. [May [cited 2015 Aug 25]; Available from: <http://www.sciencedirect.com/science/article/pii/S1226086X12003796>].
- Lei J, Yue H, Tang H, Liang B. Heat integration and optimization of hydrogen production for a 1 kW low-temperature proton exchange membrane fuel cell. *Chem Eng Sci* 2015;123:81–91. [Feb [cited 2015 Aug 25]; Available from: <http://www.sciencedirect.com/science/article/pii/S0009250914006046>].
- Li C, Gillum C, Toupin K, Donaldson B. Biomass boiler energy conversion system analysis with the aid of exergy-based methods. *Energ Convers Manage* 2015;103:665–73. [Available from: <http://linkinghub.elsevier.com/retrieve/pii/S0196890415006652>].
- Lindorfer J, Fazeni K, Steinmüller H. Life cycle analysis and soil organic carbon balance as methods for assessing the ecological sustainability of 2nd generation biofuel feedstock. *Sustain Energy Technol Assess* 2014;5:95–105. [Mar [cited 2015 Aug 5]; Available from: <http://www.sciencedirect.com/science/article/pii/S2213138813000866>].
- Liu Z, Mao Z, Xu J, Hess-Mohr N, Schmidt VM. Operation conditions optimization of hydrogen production by propane autothermal reforming for PEMFC application. *Chin J Chem Eng* 2006;14(2):259–65. [Apr, Available from: <http://linkinghub.elsevier.com/retrieve/pii/S1004954106006682>].
- Martinez-Frias J. A natural gas-assisted steam electrolyzer for high-efficiency production of hydrogen. *Int J Hydrogen Energy* 2003;28(5):483–90. [May [cited 2015 Aug 27]; Available from: <http://www.sciencedirect.com/science/article/pii/S0360319902001350>].
- Modarresi A, Wukovits W, Friedl A. Application of exergy balances for evaluation of process configurations for biological hydrogen production. *Appl Therm Eng* 2010;30(1):70–6.
- Mondal T, Pant KK, Dalai AK. Oxidative and non-oxidative steam reforming of crude bioethanol for hydrogen production over Rh promoted Ni/CeO₂-ZrO₂ catalyst. *Appl Catal A Gen* 2015;499:19–31. [Jun [cited 2015 Jul 5]; Available from: <http://www.sciencedirect.com/science/article/pii/S0926860X15002379>].
- Morales M, Quintero J, Conejeros R, Aroca G. Life cycle assessment of lignocellulosic bioethanol: environmental impacts and energy balance. *Renew Sustain Energy Rev* 2015;42:1349–61. [Feb [cited 2014 Nov 25]; Available from: <http://www.sciencedirect.com/science/article/pii/S1364032114009228>].
- Muench S, Guenther E. A systematic review of bioenergy life cycle assessments. *Appl Energy* 2013;112:257–73. [Dec [cited 2015 Jan 2]; Available from: <http://www.sciencedirect.com/science/article/pii/S03606261913005084>].
- Ni M, Leung DY, MKH L. A review on reforming bio-ethanol for hydrogen production. *Int J Hydrogen Energy* 2007;32(15):3238–47. [Oct [cited 2015 Aug 25]; Available from: <http://www.sciencedirect.com/science/article/pii/S0360319907002479>].
- Ozbilen A, Dincer I, Rosen MA. A comparative life cycle analysis of hydrogen production via thermochemical water splitting using a Cu–Cl cycle. *Int J Hydrogen Energy* 2011;36(17):11321–7. [Aug, Available from: <http://linkinghub.elsevier.com/retrieve/pii/S0360319910023773>].
- Peters JF, Iribarren D, Dufour J. Simulation and life cycle assessment of biofuel production via fast pyrolysis and hydrougrading. *Fuel* 2015;139:441–56. [Jan [cited 2015 Jun 28]; Available from: <http://www.sciencedirect.com/science/article/pii/S0016236114008746>].
- Poroch-Seritan M, Gutt S, Gutt G, Cretescu I, Cojocaru C, Severin T. Design of experiments for statistical modeling and multi-response optimization of nickel electroplating process. *Chem Eng Res Des* 2011;89(2):136–47.
- Rabenstein G, Hacker V. Hydrogen for fuel cells from ethanol by steam-reforming, partial-oxidation and combined auto-thermal reforming: a thermodynamic analysis. *J Power Sources* 2008;185(2):1293–304.
- Rahimpour MR, Dehnavi MR, Allahgholipour F, Iranshahi D, Jokar SM. Assessment and comparison of different catalytic coupling exothermic and endothermic reactions: a review. *Appl Energy* 2012;99:496–512.
- Rass-Hansen J, Johansson R, Møller M, Christensen CH. Steam reforming of technical bioethanol for hydrogen production. *Int J Hydrogen Energy* 2008;33(17):4547–54. [Sep [cited 2015 Jun 18]; Available from: <http://www.sciencedirect.com/science/article/pii/S0360319908007337>].
- Salemme L, Menna L, Simeone M. Analysis of the energy efficiency of innovative ATR-based PEM fuel cell system with hydrogen membrane separation. *Int J Hydrogen Energy* 2009;34(15):6384–92. [Aug [cited 2015 Aug 25]; Available from: <http://www.sciencedirect.com/science/article/pii/S0360319909008325>].
- Seelam PK, Liguori S, Iulianelli A, Pinacci P, Calabrò V, Huuhtanen M, et al. Hydrogen production from bio-ethanol steam reforming reaction in a Pd/PSS membrane reactor. *Catal Today* 2012;193(1):42–8. [Oct [cited 2015 Aug 25]; Available from: <http://www.sciencedirect.com/science/article/pii/S0920586112000478>].
- Simpson AP, Lutz AE. Exergy analysis of hydrogen production via steam methane reforming. *Int J Hydrogen Energy* 2007;32(18):4811–20. [Dec [cited 2015 Aug 3]; Available from: <http://www.sciencedirect.com/science/article/pii/S036031990700482X>].
- Szargut J, Morris DR, Steward FR. Exergy analysis of thermal and metallurgical processes. Hemisphere 1998.
- Tufvesson LM, Lantz M, Börjesson P. Environmental performance of biogas produced from industrial residues including competition with animal feed – life-cycle calculations according to different methodologies and standards. *J Clean Prod* 2013;53:214–23. [Aug [cited 2015 Mar 27]; Available from: <http://www.sciencedirect.com/science/article/pii/S0959652613002060>].
- Wang HM. Experimental studies on hydrogen generation by methane autothermal reforming over nickel-based catalyst. *J Power Sources* 2008;177(2):506–11. [Mar, Available from: <http://linkinghub.elsevier.com/retrieve/pii/S0378775307023671>].
- Wang L, Li N, Zhao B. Exergy performance and thermodynamic properties of the ideal liquid desiccant dehumidification system. *Energ Buildings* 2010;42(12):2437–44. [Dec [cited 2015 Aug 25]; Available from: <http://www.sciencedirect.com/science/article/pii/S0378778810002975>].